Published in final edited form as:
Horm Metab Res. 2012 September ; 44(10): 759–765. doi:10.1055/s-0032-1321866.

Prkar1a in the Regulation of Insulin Secretion

M. A. Hussain[1], **C. Stratakis**[2], and **L. Kirschner**[3]

[1]Department of Pediatrics, Medicine and Biological Chemistry, Johns Hopkins University School of Medicine, Baltimore, MD, USA

[2]National Institute of Child Health and Disease, Betheseda, MD, USA

[3]Department of Medicine, Ohio State University, Columbus, Ohio, USA

Abstract

The incidence of type 2 diabetes mellitus (T2DM) is rapidly increasing worldwide with significant consequences on individual quality of life as well as economic burden on states' healthcare costs. While origins of the pathogenesis of T2DM are poorly understood, an early defect in glucose-stimulated insulin secretion (GSIS) from pancreatic β-cells is considered a hallmark of T2DM [1]. Upon a glucose stimulus, insulin is secreted in a biphasic manner with an early first-phase burst of insulin, which is followed by a second, more sustained phase of insulin output [2]. First phase insulin secretion is diminished early in T2DM as well is in subjects who are at risk of developing T2DM [3–6].

An effective treatment of T2DM with incretin hormone glucagon-like peptide-1 (GLP-1) or its long acting peptide analogue exendin-4 (E4), restores first-phase and augments second-phase glucose stimulated insulin secretion. This effect of incretin action occurs within minutes of GLP-1/E4 infusion in T2DM humans. An additional important consideration is that incretin hormones augment GSIS only above a certain glucose threshold, which is slightly above the normal glucose range. This ensures that incretin hormones stimulate GSIS only when glucose levels are high, while they are ineffective when insulin levels are below a certain threshold [7, 8]. Activation of the GLP-1 receptor, which is highly expressed on pancreatic β-cells, stimulates 2 distinct intracellular signaling pathways: a) the cAMP-protein kinase A branch and b) the cAMP-EPAC2 (EPAC = exchange protein activated by cAMP) branch. While the EPAC2 branch is considered to mediate GLP-1 effects on first-phase GSIS, the PKA branch is necessary for the former branch to be active [9, 10]. However, how these 2 branches interplay and converge and how their effects on insulin secretion and insulin vesicle exocytosis are coordinated is poorly understood. Thus, at the outset of our studies we have a poorly understood intracellular interplay of cAMP-dependent signaling pathways, which – when stimulated – restore glucose-dependent first phase and augment second phase insulin secretion in the ailing β-cells of T2DM.

Correspondence. ***M. A. Hussain***, Department of Pediatrics, Medicine and Biological Chemistry, Johns Hopkins University, 600 North Wolfe Street, Baltimore, MD 21287, USA, Tel.: + 1/410/5025 770, Fax: + 1/410/5025 779, mhussai4@jhmi.edu.

Conflict of Interest

The authors have no conflict of interest to disclose.

Keywords

type 2 diabetes; Prkar1a; insulin secretion

Disinhibition of PKA in β-Cells

To examine in detail the role of the cAMP-PKA branch of incretin signaling in pancreatic β-cells, we disinhibited PKA signaling by way of ablating in vivo in mice the most abundantly expressed PKA regulatory subunit prkar1a (Fig. 1) [11]. Pancreas-specific PDX-1 CRE mice interbred with floxed prkar1a mice yielded off spring in the expected Mendelian frequency with no obvious phenotype on simple observation. Fasting glucose and insulin levels were not remarkably different between Δ-prkar1a and control littermates. However, upon glucose stimulation during intra-peritoneal glucose tolerance tests (ipGTT), Δ-prkar1a mice showed significantly blunted glucose excursions, while insulin secretion was approx 8- to 10-fold augmented. In addition, it appeared that the first phase of insulin secretion was potently augmented in Δ-prkar1a (Fig. 2). Further analysis revealed that increased insulin secretory capacity of Δ-prkar1a mice was not due to increased β-cell mass (Fig. 3), indicating that prkar1a ablation and PKA disinhibition in β-cells primarily augments glucose-dependent insulin secretion.

Humans with inactivating Prkar1a mutations (Carney's complex) also showed during oral GTT increased insulin excursions, while plasma glucose excursion were blunted as compared to controls with similar medical history but without prkar1a mutations (Fig. 4). It should be noted that the human phenotype is in the heterozygous state and the glucose tolerance tests are via oral administration as compared to the ivGTT in homozygous Δ-prkar1a mice. These differences may explain the somewhat subtle phenotype in humans as compared to Δ-prkar1a mice.

PKA Target Snapin Integrates β-Cell cAMP Pathways Stimulating Insulin Exocytosis

Ultrastructural analysis of Δ-prkar1a β-cells showed an increased number of insulin vesicles lined adjacent to the plasma membrane in the vicinity of intra-islet capillaries. Insulin vesicles in this location were also larger in size than vesicles located further in the interior of the β-cell (Fig. 5). This observation led us to further explore potential PKA targets, which may be involved in vesicle exocytosis.

An in silico search in multiple databases for PKA target proteins involved in vesicle exocytosis repeatedly indentified the small adaptor protein snapin as a strong candidate. Snapin is a direct target of PKA and mediates neuronal synaptic exocytosis [12]. In neuronal cells snapin is phosphorylated at serine 50 in a PKA-dependent manner and upon phosphorylation interacts with SNAP25, a core component of the SNARE complex located at the inner face of the cell plasma membrane. Importantly, snapin is also enriched at high levels in pancreatic β-cells [13] (Fig. 6a) and its phosphorylation is stimulated by E4 in a PKA-dependent manner in mouse and human islets (Fig. 6b, c).

Similar to the findings in neuronal cells, in β-cells snapin is phosphorylated in a PKA-dependent manner at serine 50, which is flanked by a PKA consensus sequence. S50 snapin phosphorylation increases its interaction with SNAP25 as well as with EPAC2 (Fig. 7a) resulting in the formation of a protein hetero-complex, which is required for insulin exocytosis. Thus it appears that in β-cells phosphorylated snapin serves as a node, where PKA independent (cAMP-EPAC2) and PKA dependent (S50 phospho-snapin) incretin effects converge.

A mutant isoform of snapin with serine 50 altered to aspartate (snapin S50D), which mimics snapin S50 phosphorylation, allows formation of a hetero-complex between snapin, SNAP25 and EPAC2 (Fig. 7b). Complete assembly of the SNARE complex leading to vesicle exocytosis requires the interaction of proteins bound to the inner surface of the plasma membrane (membrane bound SNARE proteins) with proteins attached to the secretory vesicle (vesicle bound SNARE proteins, i. e., VAMP2) through a hand-shake of coiled-coiled motifs on both sides. Snapin interacts with the membrane bound protein SNAP25 in a S50D-dependent manner and promotes assembly of vesicle associated proteins, preparing the secretory vesicle for exocytosis. Finally, elevated glucose levels promote – most likely in a Ca^{2+} dependent manner – snapin interaction with the vesicle-associated protein VAMP2 (Fig. 7c). This observation provides a basis for the glucose-dependency of incretin hormone action, in which incretin hormones (via cAMP-PKA and -EPAC2) are ineffective at low glucose levels.

Introduction in mouse islets of the snapin S50D mutant by adenovirus-mediated transduction, resulted in augmented first and second phase GSIS, similar to the effects found by E4 stimulation (Fig. 7d).

Snapin S50 is O-GlcNAcylated in T2DM and PKA Mediated Snapin S50 Phosphorylation Restores First Phase and Augments Second Phase Insulin Secretion in Diabetic Islets

What then is it about the pancreatic β-cell in T2DM with β-cell dysfunction and loss of first phase GSIS, which is so effectively and rapidly (within minutes; see above) reversed by incretin pharmacotherapy?

Protein function and confirmation occur rapidly with post-translational modification. Hyperglycemia and T2DM are associated with increased post-translational protein modification with O-linked β-N-acetylglucosamine residues (O-GlcNAcylation) in peripheral tissues as well as in pancreatic islets [14]. Islet protein O-GlcNAcylation is associated with reduced insulin secretion [15]. Enzymes regulating O-GlcNAcylation, O-GlcNAc transferase and O-GlcNAcase are expressed at high levels in pancreatic islets [14, 16]. Furthermore, protein modifications at serine and threonine can alternate between phosphorylation and O-GlcNAcylation, and addition and removal of O-GlcNAc moieties cycle rapidly [17].

Based on these considerations, we examined whether snapin may be O-GlcNAcylated in diabetic islets and whether E4 treatment may influence snapin O-GlcNAcylation in a time

frame, which is consistent with clinical observations of rapid incretin effects on GSIS. In islets of mice rendered glucose intolerant with a high fat content diet (diet induced obesity and diabetes = DIO diabetes) [18], islet snapin was indeed hyper-O-GlcNAcylated as compared to control islets (Fig. 8a). Mapping of the O-GlcNacylation site on snapin revealed that in DIO diabetic islets, snapin is O-GlcNAcylated at snapin S50 (Fig. 8b). Furthermore, E4 treatment of DIO diabetic islets reversed snapin O-GlcNAcylation to benefit snapin phosphorylation (Fig. 8c). Thus, it appears that in T2DM snapin S50 is the target of O-GlcNAcylation, which is rapidly reversed by E4, by way of a PKA-dependent snapin S50 phosphorylation.

Finally, introduction of snapin S50D mutant, which is impervious to O-GlcNAcylation restores first and second phase insulin secretion in DIO diabetic islets (Fig. 8d).

Summary

These findings indicate the important role of prkar1a in regulating PKA-mediated pancreatic β-cell insulin secretion. The roles in β-cells for the other PKA regulatory subunits remain to be examined. In addition our findings provide a model of how the incretin-activated cAMP-PKA and cAMP-EPAC2 signaling pathways are integrated towards insulin secretion.

Our findings suggest that snapin S50 phosphorylation provides unifying mechanism for the following properties of incretin action: (1) glucose dependency in augmenting insulin secretion; (2) rapid action of GLP-1 and E4 in stimulating first- and second phase insulin secretion, and (3) rapid effectiveness in DIO diabetic islets in restoring first- and second phase insulin secretion, by altering the proportion of phosphorylated to O-GlcNAcylated snapin S50.

Both prkar1a and snapin are targets for potential pharmacologic drug development for T2DM.

Acknowledgments

Supported by an Endocrine Society Student Research Fellowship (MAH), Eunice Kennedy Shriver National Institutes of Child Health and Human Development Intramural Program (CAS), National Institutes of Health (NIH) CA112268 (LSK), DK81472, DK63349, DK84948 and DK79637 (MAH).

Fig. 1–8 were reproduced from reference [19] by the authors.

References

1. Nolan CJ, Damm P, Prentki M. Type 2 diabetes across generations: from pathophysiology to prevention and management. Lancet. 2011; 378:169–181. [PubMed: 21705072]
2. Del Prato S, Tiengo A. The importance of first-phase insulin secretion: implications for the therapy of type 2 diabetes mellitus. Diabetes Metab Res Rev. 2001; 17:164–174. [PubMed: 11424229]
3. Gerich JE. Is reduced first-phase insulin release the earliest detectable abnormality in individuals destined to develop type 2 diabetes? Diabetes. 2002; 51(Suppl 1):S117–S121. [PubMed: 11815469]
4. Lillioja S, Mott DM, Howard BV, Bennett PH, Yki-Jarvinen H, Frimond D, Nyomba BL, Zurlo F, Swinburn B, Bogardus C. Impaired glucose tolerance as a disorder of insulin action. Longitudinal and cross-sectional studies in Pima Indians. N Engl J Med. 1988; 318:1217–1225. [PubMed: 3283552]

5. Vaag A, Henriksen JE, Madsbad S, Holm N, Beck-Nielsen H. Insulin secretion, insulin action, and hepatic glucose production in identical twins discordant for non-insulin-dependent diabetes mellitus. J Clin Invest. 1995; 95:690–698. [PubMed: 7860750]
6. Ward WK, Bolgiano DC, McKnight B, Halter JB, Porte D Jr. Diminished B cell secretory capacity in patients with noninsulin-dependent diabetes mellitus. J Clin Invest. 1984; 74:1318–1328. [PubMed: 6384269]
7. Egan JM, Clocquet AR, Elahi D. The insulinotropic effect of acute exendin-4 administered to humans: comparison of nondiabetic state to type 2 diabetes. J Clin Endocrinol Metab. 2002; 87:1282–1290. [PubMed: 11889200]
8. Fehse F, Trautmann M, Holst JJ, Halseth AE, Nanayakkara N, Nielsen LL, Fineman MS, Kim DD, Nauck MA. Exenatide augments first- and second-phase insulin secretion in response to intravenous glucose in subjects with type 2 diabetes. J Clin Endocrinol Metab. 2005; 90:5991–5997. [PubMed: 16144950]
9. Drucker DJ. The biology of incretin hormones. Cell Metab. 2006; 3:153–165. [PubMed: 16517403]
10. Drucker DJ, Nauck MA. The incretin system: glucagon-like peptide-1 receptor agonists and dipeptidyl peptidase-4 inhibitors in type 2 diabetes. Lancet. 2006; 368:1696–1705. [PubMed: 17098089]
11. Petyuk VA, Qian WJ, Hinault C, Gritsenko MA, Singhal M, Monroe ME, Camp DG 2nd, Kulkarni RN, Smith RD. Characterization of the mouse pancreatic islet proteome and comparative analysis with other mouse tissues. J Proteome Res. 2008; 7:3114–3126. [PubMed: 18570455]
12. Chheda MG, Ashery U, Thakur P, Rettig J, Sheng ZH. Phosphorylation of Snapin by PKA modulates its interaction with the SNARE complex. Nat Cell Biol. 2001; 3:331–338. [PubMed: 11283605]
13. Fukui K, Yang Q, Cao Y, Takahashi N, Hatakeyama H, Wang H, Wada J, Zhang Y, Marselli L, Nammo T, Yoneda K, Onishi M, Hagashiyama S, Matsuzawa Y, Gonzalez FJ, Weir GC, Kasai H, Shimomura I, Miyagawa J, Wollheim CB, Yamagata K. The HNF-1 target collectrin controls insulin exocytosis by SNARE complex formation. Cell Metab. 2005; 2:373–384. [PubMed: 16330323]
14. Copeland RJ, Bullen JW, Hart GW. Cross-talk between GlcNAcylation and phosphorylation: roles in insulin resistance and glucose toxicity. Am J Physiol Endocrinol Metab. 2008; 295:E17–E28. [PubMed: 18445751]
15. Akimoto Y, Hart GW, Wells L, Vosseller K, Yamamoto K, Munetomo E, Ohara-Imaizumi M, Nishiwaki C, Nagamatsu S, Hirano H, Kawakami H. Elevation of the post-translational modification of proteins by O-linked N-acetylglucosamine leads to deterioration of the glucose-stimulated insulin secretion in the pancreas of diabetic Goto-Kakizaki rats. Glycobiology. 2007; 17:127–140. [PubMed: 17095531]
16. Wang Z, Udeshi ND, Slawson C, Compton PD, Sakabe K, Cheung WD, Shabanowitz J, Hunt DE, Hart GW. Extensive crosstalk between O-GlcNAcylation and phosphorylation regulates cytokinesis. Sci Signal. 2010; 3:ra2. [PubMed: 20068230]
17. Zeidan Q, Hart GW. The intersections between O-GlcNAcylation and phosphorylation: implications for multiple signaling pathways. J Cell Sci. 2010; 123:13–22. [PubMed: 20016062]
18. Peyot ML, Pepin E, Lamontagne J, Latour MG, Zarrouki B, lussier R, Pineda M, Jetton TL, Madiraju SR, Joly E, Prentki M. Beta Cell Failure in Diet-Induced Obese mice stratified according to body weight gain: secretory dysfunction and altered islet lipid metabolism without steatosis or reduced beta cell mass. Diabetes. 2010; 59:2178–2187. [PubMed: 20547980]
19. Song WJ, Seshadri M, Ashraf U, Mdluli T, Mondal P, Keil M, Azevedo M, Kirschner LS, Stratakis CA, Hussain MA. Snapin mediates incretin action and augments glucose-dependent insulin secretion. Cell Metab. 2011; 13:308–319. [PubMed: 21356520]

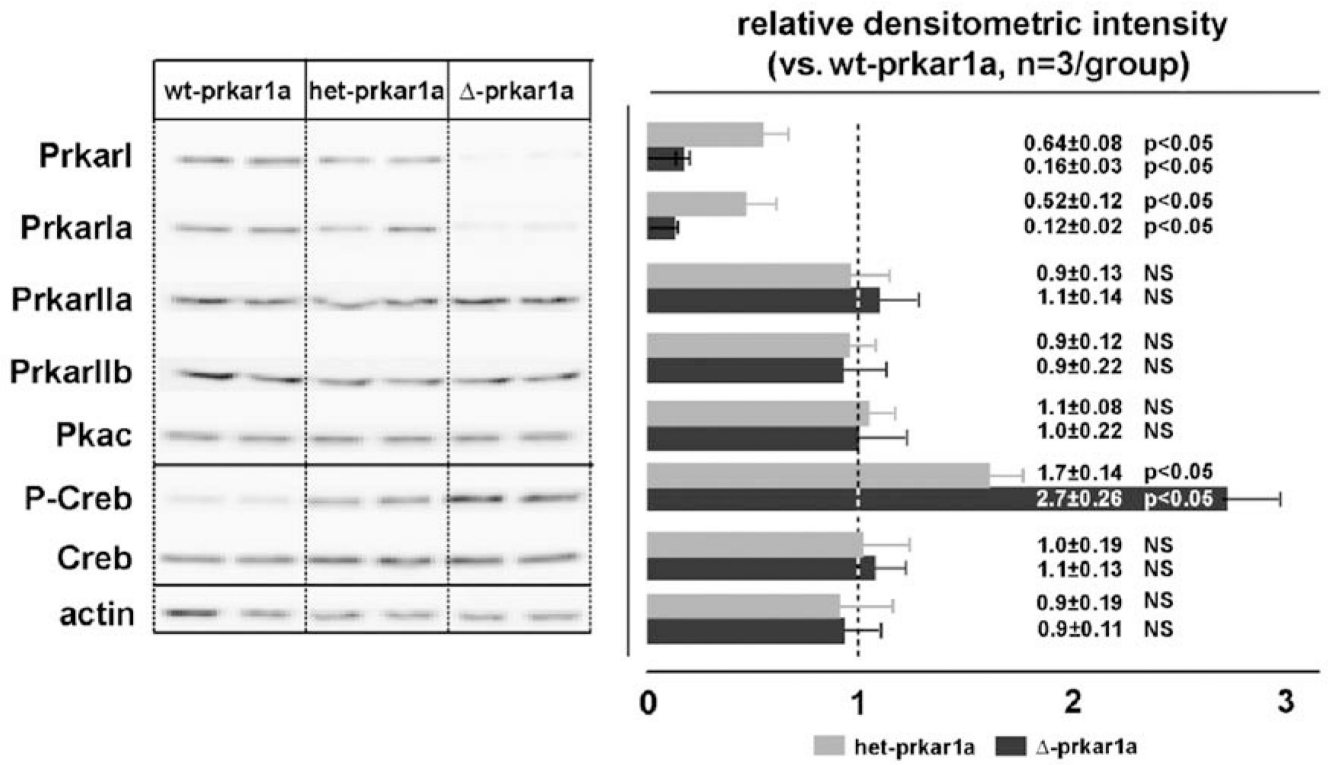

Fig. 1.

Prkar1a ablation in pancreatic islets. Immunoblot (left) with densitometric analysis (right) of total islet protein from wt-prkar1a, hetprka1a, Δ-prkar1a mice. Specific Prkar1a ablation is detectable, while other prkar subtypes and Pkac remain unchanged. Total prkar1a reduction reflects predominant prkar1a expression in β-cells. Prkar1a expression is approximately 50 % reduced in het-prkar1a islets and 90 % reduced in Δ-rkar1a islets. CREB phosphorylation increases with reduced Prkar1a abundance. Reproduced with kind permission of Elsevier.

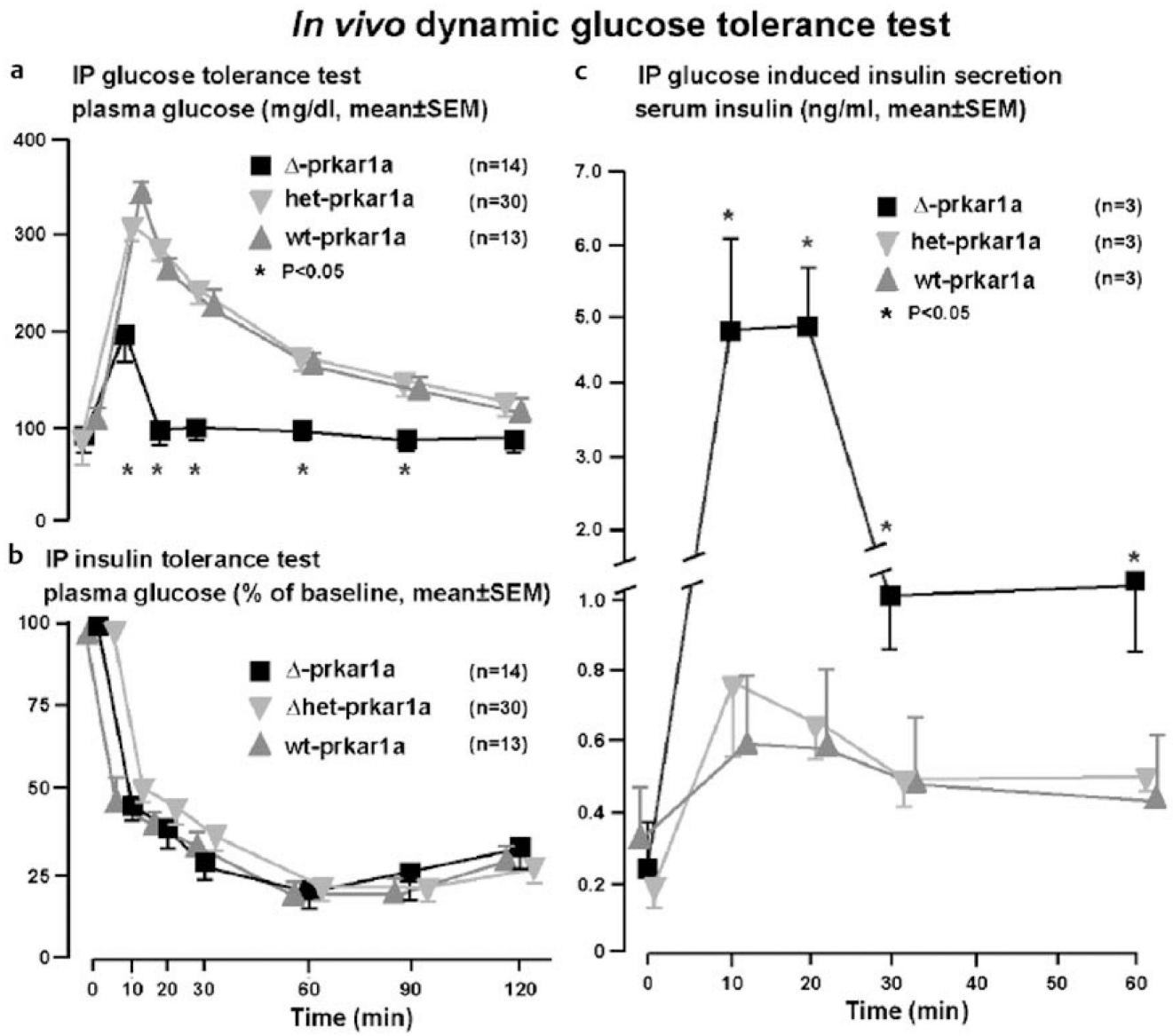

Fig. 2.

Glucose stimulated insulin secretion in Δ-prkar1a, het-prkar1a, and wt-prkar1a mice in vivo and from respective mouse islets in vitro. **a** Plasma glucose levels during an ipGTT in littermates of indicated genotypes. Δ-Prkar1a mice have markedly diminished glucose excursion during ipGTT but do not exhibit baseline or post glucose hypoglycemia (*$p < 0.05$). **b** Plasma glucose levels during ipITT in littermates of indicated genotypes. No difference is seen in insulin sensitivity among the different genotypes (*$p < 0.05$). **c** Serum insulin levels during ipGTT in littermates of indicated genotypes. All animals have similar baseline insulin levels. Δ-Prkar1a mice have markedly increased glucose stimulated insulin levels, predominantly during the initial phases of ipGTT (*$p < 0.05$). Reproduced with kind permission of Elsevier.

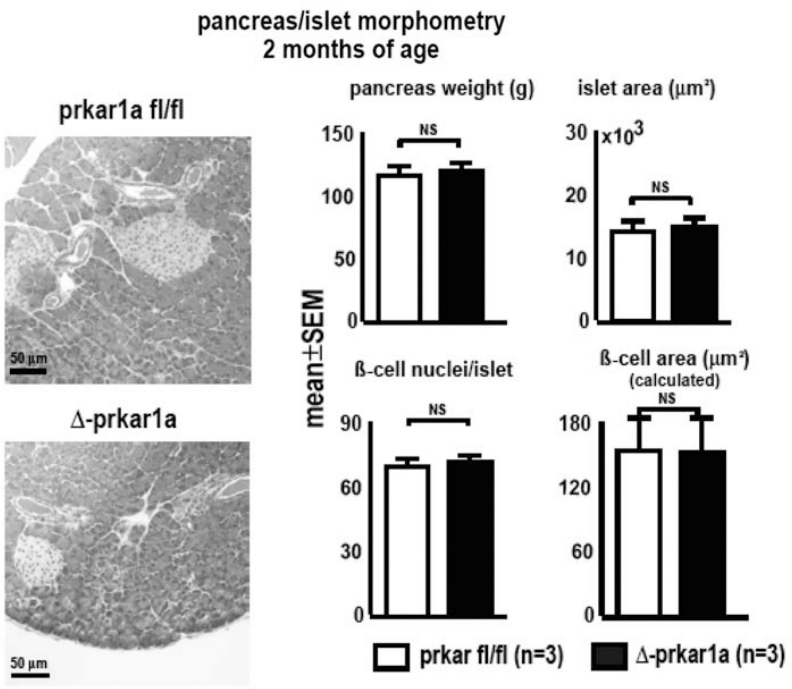

Pancreas morphometric parameters (islet area, ß-cells/islet, ß-cell size), proliferation indices (Ki67. Edu incorporation) and islet insulin content of genotype complements derived from pdx1-CRE/prkar1a $^{fl/fl}$ breeding. Data are from 8-9 months old animals. No significant differences are found between !-prkar1a mice and the other genotype complements. All parameters are given in mean±SEM; n=3 in each genotype group.

	wt-prkar1a	het-prkar1a	!-prkar1a
Parameter (Mean±SEM)			
Islet area ($\mu m^2 x10^3$)	14.26±0.76	14.38±0.81	14.5±0.80
ß-cell nuclei/islet	85.4±4.8	88.3±4.9	87.1±4.7
ß-cell size (μm^2)	169.1±2.1	163.6±2.1	166.4±0.7
Ki67+ ß-cells (% of all ß-cells)	3.5±0.12	3.6±0.26	3.4±0.15
EdU + ß-cells (% of all ß-cells)	4.6±0.20	5.3±0.33	5.9±0.44
Islet insulin (ng/islet $x10^2$)	2.2±0.2	2.1±0.5	1.9±0.4

Fig. 3.

Δ-Prkar1a mice do not show any change in islet mass or β-cell proliferation. Top panel: Representative photomicrographs of Δ-prkar1a and control pancreata and morphometric analyses of pancreatic β-cells. Bottom panel: Pancreas morphometric analyses of control, heterezygote and Δ-prkar1a mice confirm no changes in islet cell mass in Δ-prkar1a mice. Reproduced with kind permission of Elsevier.

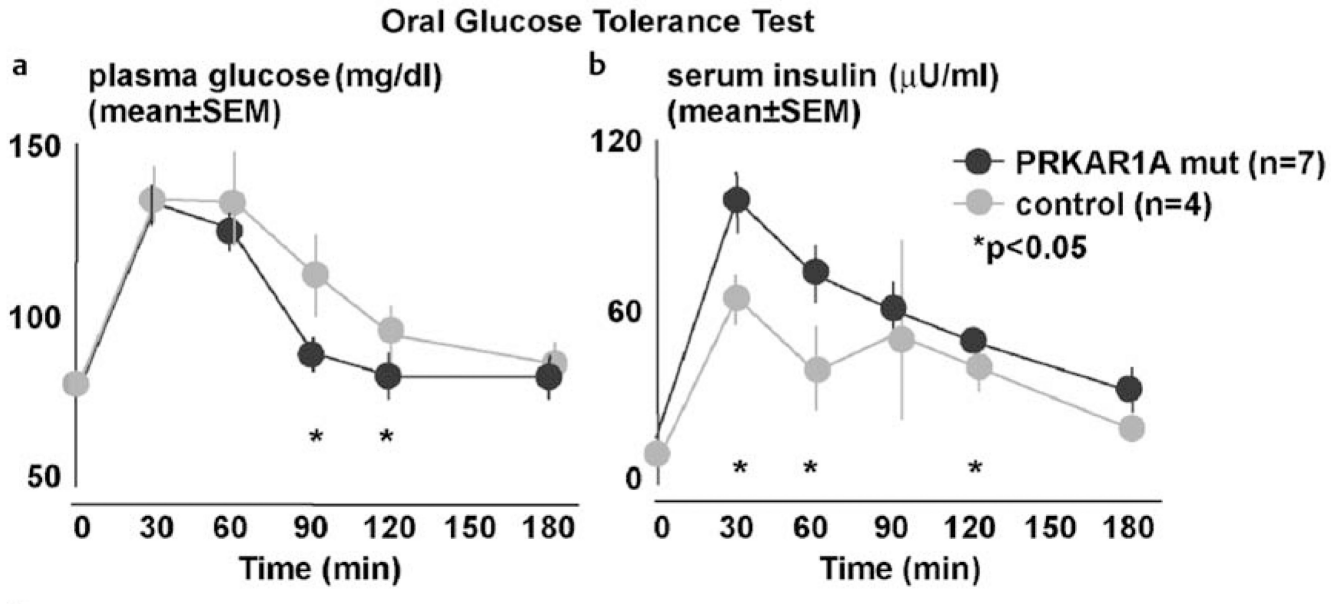

c

	PRKAR1A mut	control	Non-parametric test (Mann-Whitney U)
Glucose Fasting (mg/dl)	76±12	78±15	NS
AUC (mg/dl*min) during oGTT	4 185±136	5 260±149	p<0.05
Insulin Fasting (mU/ml)	14±5	4.6±9	NS
AUC (mU/ml*min) During oGTT	7 707±241	6 138±211	p<0.05

Fig. 4.

Oral GTT after in humans with inactivating *PRKAR1A* mutations and controls. **a** Subjects with a *PRKAR1A* mutation exhibit normal fasting glucose levels but reduced glucose excursion after an oral glucose load. **b** In subjects with a *PRKAR1A* mutation serum insulin levels were not different at baseline, and reached a higher peak with increased overall insulin secretion. **c** Table summarizing fasting glucose and insulin levels as well as area under the glucose and insulin curves shown in **a** and **b** (*p < 0.05). Reproduced with kind permission of Elsevier.

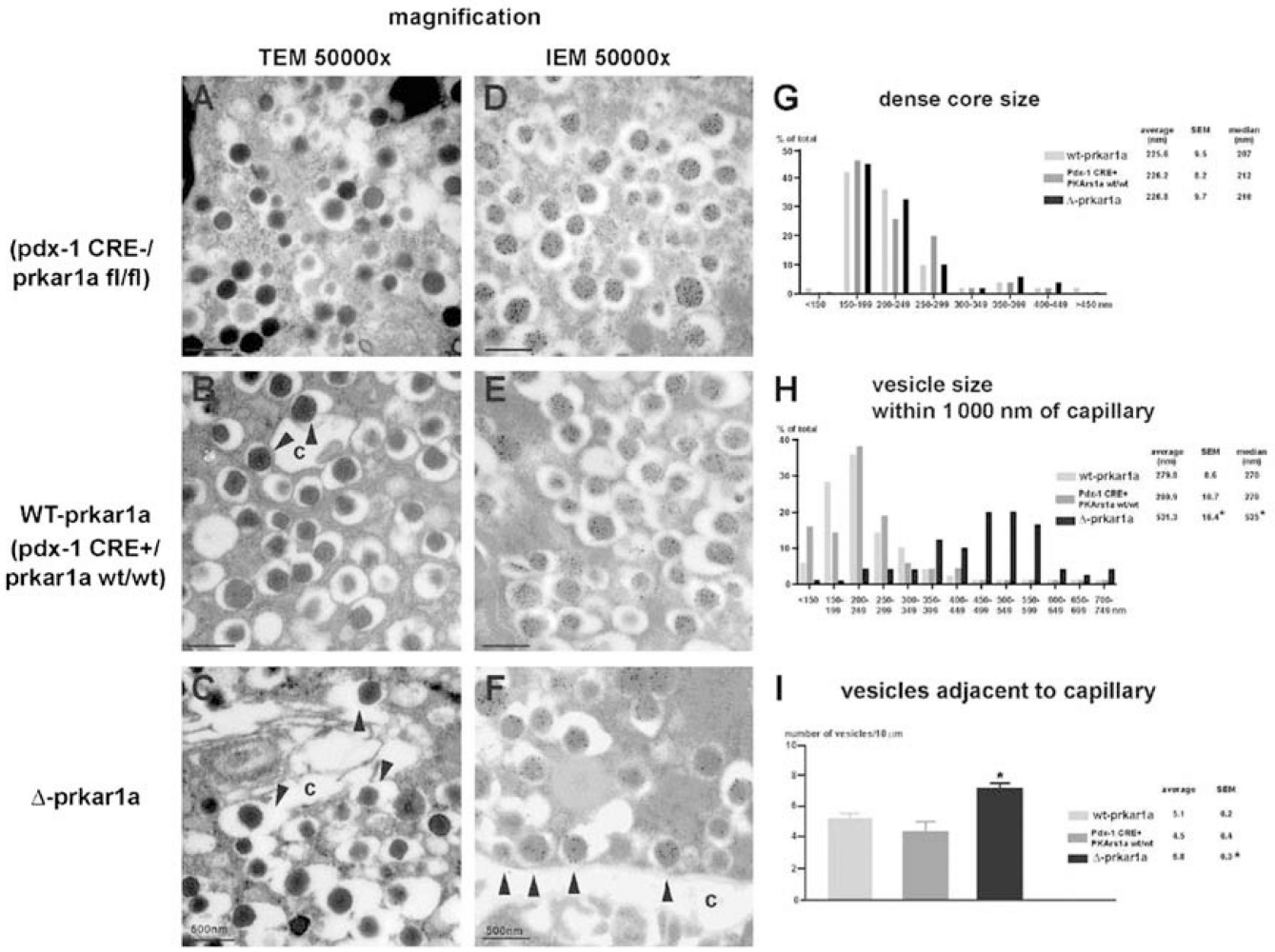

Fig. 5.

Representative electron microscopic images of islets (**A, B**: 50 000 × magnification of transmission EM; **C**, **D** Immuno EM microscopy for insulin detection, 50 000 × magnification) of wt-prkar1a (top) and Δ-prkar1a (bottom) littermates. Δ-Prkar1a islets exhibit increased vesicle size in proximity of intraislet capillaries, while dense cores containing insulin are unchanged. Panels **A** and **B** show capillaries (denoted by "c") with insulin vesicles along the capillary border (arrowheads). **E** Dense core size distribution in percent of total vesicles viewed. No difference between the various genotypes is observed (mean ± SEM). **F** Size distribution of insulin vesicles within 1 000 nm of capillaries in percent of total vesicles observed. Δ-Prkar1a exhibit significantly larger vesicles (mean ± SEM, * signifies $p < 0.05$). **G** Number of insulin vesicles aligned along intra-islet capillary/ 10 μm of plasma membrane length. Δ-Prkar1a β-cells show significantly more vesicles adjacent to capillaries (mean ± SEM, * signifies $p < 0.05$). Reproduced with kind permission of Elsevier.

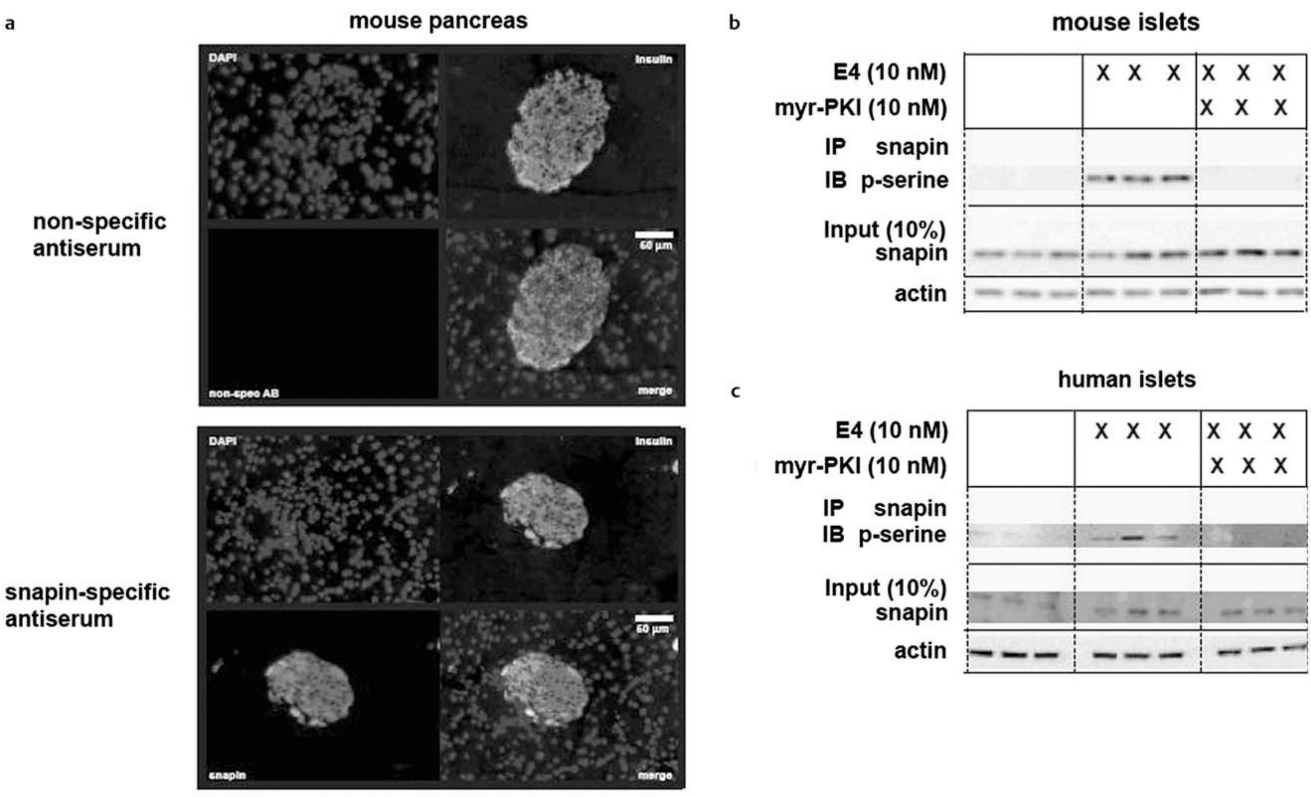

Fig. 6.

a Immunohistochemical staining of mouse pancreas sections. Co-immunostaining with insulin (green) and with nonspecific antibody (top) or snapin-specific antibody (bottom) (red). Nuclear counterstain with DAPI (blue). Separate pseudocolored images are shown with digitally merged image on bottom right panel, respectively. Snapin immunoreactivity co-localizes with insulin immunoreactivity in pancreatic islets. **b** Co-immunoprecipitation for snapin serine phosphorylation in mouse islets treated with E4 without or with PKA specific inhibition with myr-PKI. E4 stimulates snapin phosphorylation, which is inhibited by adding myr-PKI. Immunoblot for 10 % of protein input at bottom. **c** Co-immunoprecipitation for snapin serine phosphorylation in human islets treated with E4 (10 nM) without or with PKA specific inhibition with myr-PKI. E4 stimulates snapin phosphorylation, which is inhibited by adding myr-PKI. Immunoblot for 10 % of protein input at bottom. Reproduced with kind permission of Elsevier.

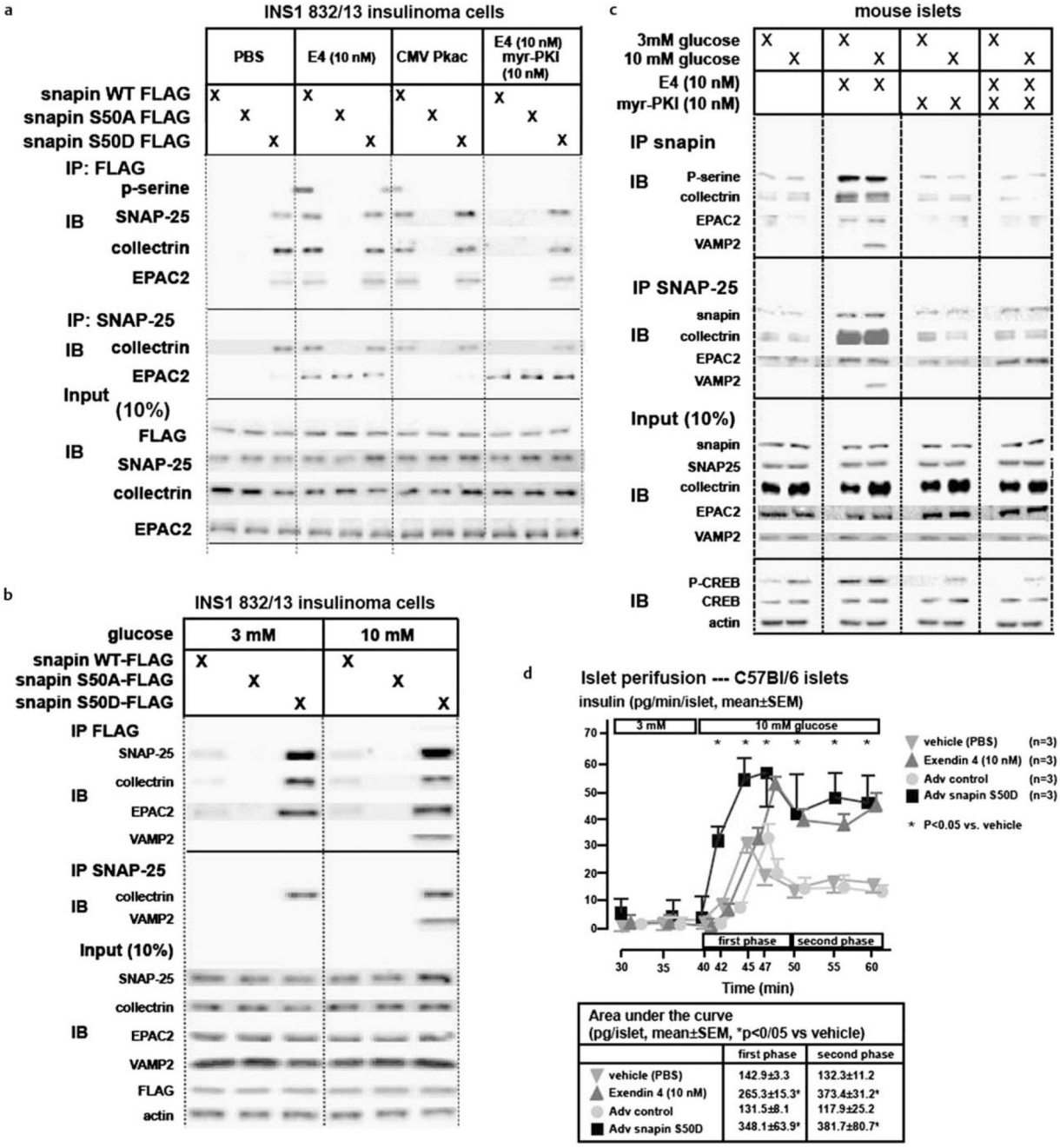

Fig. 7.

PKA mediated phosphorylation of snapin maps to serine 50. Snapin S50 phosphorylation increases interaction with secretory vesicle-associated proteins SNAP-25, EPAC2 and collectrin. Snapin interaction with VAMP2 is glucose dependent. E4 stimulated SNAP-25 interaction with EPAC2 is not PKA mediated. Overexpression in islets of snapin S50D potentiates GSIS. **a** Transiently transfected INS1 832/13 cells expressing C-terminal FLAG tagged WT, S50A or S50D snapin were treated with PBS (vehicle) E4 (10 nM), myr-PKI (10 nM), treated E4 + myr-PKI, or transfected with Pkac followed by IP for FLAG or

SNAP-25 and IB for phosphoserine or interacting proteins. Snapin serine phosphorylation occurs in WT snapin and not in S50A and S50D mutants by E4 and Pkac action. E4 effect is inhibited by myr-PKI. Snapin interaction with SNAP-25, collectrin or EPAC2 occurs only with phosphorylated WT snapin (by E4 or Pkac) or with snapin S50D as does SNAP-25 interaction with collectrin. SNAP-25 interaction with EPAC2 occurs with E4 in a PKA-independent manner and not inhibited by myr-PKI. **b** Transiently transfected INS1 832/13 cells expressing C-terminal FLAG tagged WT, S50A or S50D snapin cultured in low (3 mM) or high (10 mM) glucose and co-IP/IB as in **a**. Snapin S50D mutant binds SNAP-25, collectrin and EPAC2 in both low and high glucose. Snapin interaction with VAMP2 occurs at elevated glucose levels only. SNAP-25-VAMP2 interaction occurs only with snapin S50D and at elevated glucose levels. **c** Isolated C57Bl/6 mouse islets cultured in low (3 mM) or high (10 mM) glucose and treated with PBS, E4 (10 nM), myr-PKI (10 nM) and E4 + myr-PKI followed by co-IP/IB as in **a**. Snapin serine phosphorylation is stimulated by E4 in a PKA dependent manner and increases snapin interaction with SNAP-25, collectrin and EPAC2 independently of glucose levels. Snapin-VAMP2 interaction is stimulated by E4 in PKA dependent manner only with high glucose. E4 stimulates SNAP25-EPAC2 interaction in a glucose- and PKA-independent manner. SNAP-25-VAMP2 interaction is stimulated by E4 in a glucose and PKA-dependent manner. PKA activity is verified by phosphorylation of CREB at serine 133 (p-CREB). **d** Perifusion studies of C57Bl/6 mouse islets in low (3 mM) followed by high (10 mM) glucose concentrations. Islets were treated with either PBS (inverted triangle), E4 (10 nM) (upright triangle) during perifusion, or had been transduced with control (circle) or snapin S50D (square) expressing adenovirus. Table below the curve summarizes area under the curves for first and second phase insulin secretion (*$p < 0.05$ vs. vehicle). Reproduced with kind permission of Elsevier.

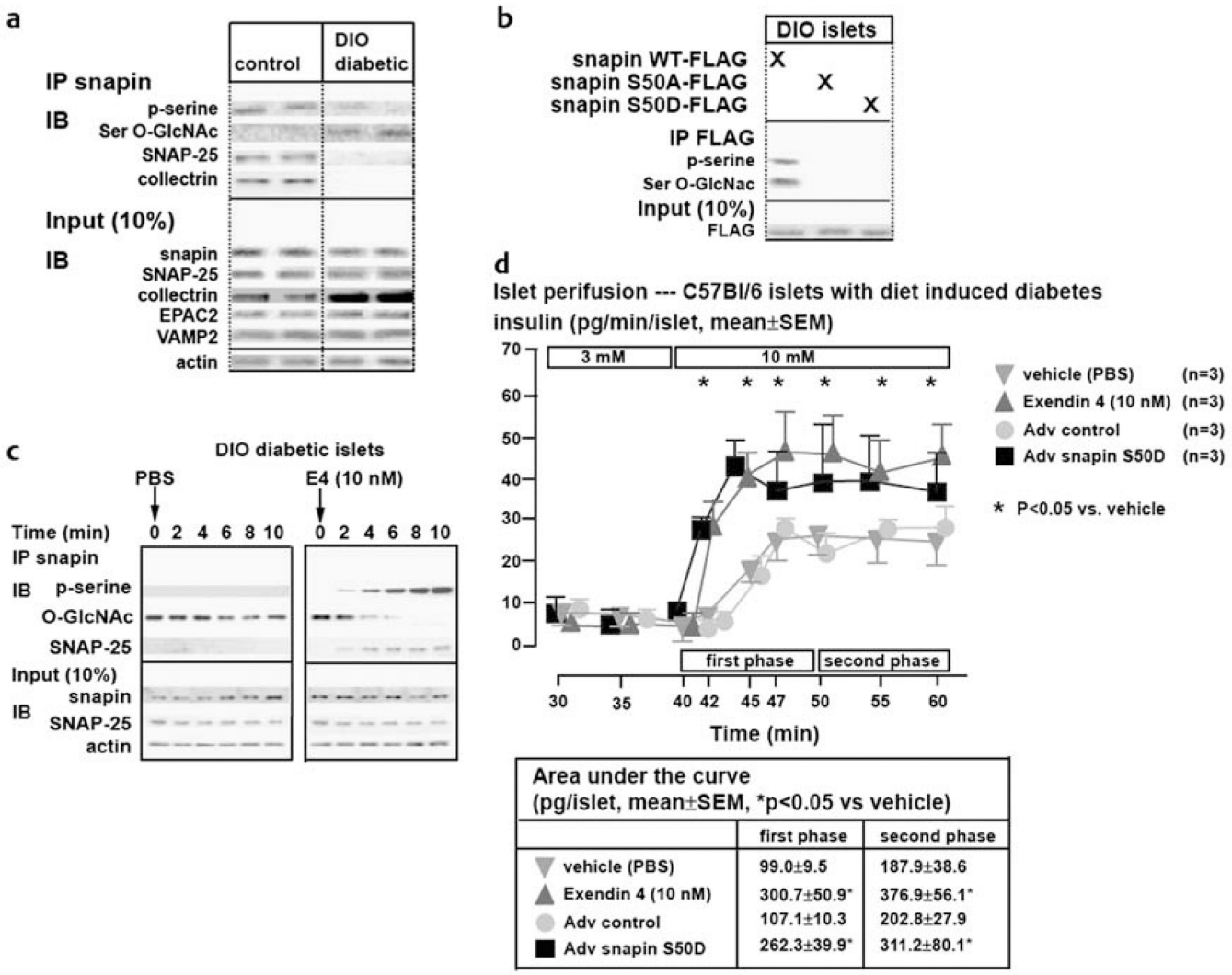

Fig. 8.

Impaired GSIS in DIO diabetic mouse islets is corrected with snapin S50D. **a** Immunoblot of islet proteins from C57Bl/6 mice on normal chow and high fat diet. **b** Mapping of snapin serine-O-GlcNAcylation. DIO diabetic islets were transduced with adenovirus expressing C-terminal FLAG-tagged wild-type, S50A and S50D snapin isoforms. Immunoprecipitation with FLAG antibody followed by immunoblot was performed. Representative immunoblot is shown. Bar graph indicates densitometric analysis of 3 separate studies. **c** Time course of snapin phosphorylation after E4 treatment of cultured islets of diet induced diabetic mice. **d** Perifusion studies of DIO mouse islets in low (3 mM) followed by high (10 mM) glucose concentrations. Islets were treated with either PBS (inverted triangle), E4 (10 nM) (upright triangle) during perifusion, or had been transduced with control (circle) or snapin S50D (square) expressing adenovirus. Table below the curve summarizes area under the curves for first and second phase insulin secretion (*p < 0.05 vs. vehicle). Reproduced with kind permission of Elsevier.